COMMUNICATION

Check for updates

Phenoxazine-based small molecule heterojunction nanoparticles for photocatalytic hydrogen production†

Mariia V. Pavliuk, [ID] Sina Wrede [ID] and Haining Tian [ID] *

A phenoxazine-based small organic molecular donor POZ-M is designed and synthesized to prepare organic heterojunction nanoparticles (NPs) with a small molecular acceptor ITIC for photocatalytic hydrogen production, giving a reaction rate of up to 63 mmol g^{-1} h^{-1}. A beneficial molecular design strategy highlights the role of miscibility between POZ-M and ITIC, which is necessary to achieve satisfactory charge separation at the donor/acceptor interface.

In order to eliminate the effects of global warming, and current economic dependence on fossil fuels that have shaken the foundation of peace worldwide, nonrenewable energy sources must be urgently replaced with sustainable alternatives. Efficient accumulation of solar energy in the form of fuels, *e.g.* hydrogen, offers the possibility of its transportation and conversion to electricity, heat or valuable goods on demand. The field of photocatalysis has largely expanded in solar fuel research in the last few years, and now organic photocatalysts are of growing interest due to their biocompatibility and ability to work with various (co-)catalysts to generate a wide range of valuable products from water, CO_2 and sunlight, *e.g.* H_2,[1–8] H_2O_2,[9–11] formate,[9] poly-3-hydroxybutyrate,[12] acetate,[13] 2-oxobutyrate,[14] *etc.*

Typically, high exciton binding energies limit the spontaneous exciton dissociation of organic photocatalysts. Thus, the subsequent short exciton diffusion distances hinder excitons from reaching the surface, and from dissociation to free charge carriers that should participate in desired chemical transformations.[15] Heterojunction nanoparticle (NP) design has been approved to be a good strategy to enhance the generation of free charge carriers, but to date, either the donor or the acceptor part of heterojunction NPs comprised organic polymers.[4,7,16,17] Recently, several works used small molecule NPs that showed impressive external quantum efficiencies even in the absence of polymeric donors.[5,6,18–20]

Small molecules offer highly tunable molecular structure, band gap and energy levels. And in contrast to most polymers, small molecules demonstrated the ability to form favorable morphology with highly crystalline networks that may offer efficient generation of free carriers, and thus suppressed recombination rates.[4] This becomes feasible due to aligned transition dipole moments in the crystal structure as well as small energetic disorders.[21]

Even though several promising single molecule examples of organic photocatalysts have been presented to date, no exclusively small molecular heterojunction architectures have been introduced to the best of our knowledge. Having both molecular donor and molecular acceptor parts with a good interaction within the heterojunction may result in enhanced charge separation and delocalization which could benefit photocatalytic reactions. In this work, a phenoxazine-based small molecular donor is therefore designed and synthesized to prepare molecular heterojunction NPs with a small molecular acceptor, ITIC, for photocatalytic hydrogen evolution.

Fig. 1a illustrates the chemical structures of small molecules POZ-M and ITIC used for the preparation of heterojunction NPs. The phenoxazine (POZ) unit has a good electron-donating ability, is facilely tuned from the structure, and is therefore used in this work to synthesize POZ-M as a small organic donor. In this donor molecule two thiophene π units are covalently linked to the phenoxazine core and two aldehyde units act as electron-withdrawing units to increase intramolecular charge separation, making the absorption of its particle form located into the visible light region up to 550 nm (Fig. 1c). Details of the synthetic procedure and characterization of POZ-M can be found in the ESI† (Fig. S1–S3). Acceptors that are prone to form crystalline architectures in NPs, such as ITIC, have shown a positive impact on charge separation with polymer donors.[17] Additionally, ITIC has absorption of its nanoparticle form from 520 nm to 700 nm which is complementary to the absorption of POZ-M NPs, 400–570 nm. Therefore, ITIC is selected as a small organic acceptor to prepare heterojunction NPs together with POZ-M.

Using the amphiphilic surfactant PS-PEG-COOH, heterojunction small molecule NPs were synthesized *via* the

Department of Chemistry-Ångström Laboratory, Physical Chemistry, Uppsala University, Uppsala, Sweden. E-mail: haining.tian@kemi.uu.se

† Electronic supplementary information (ESI) available: Synthesis of materials and their detailed characterization. See DOI: https://doi.org/10.1039/d3cc01013a
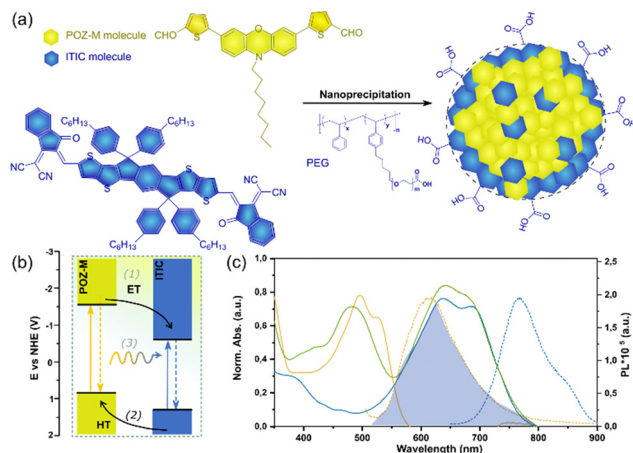
Fig. 1 (a) Chemical structures of POZ–M and ITIC used for the preparation of heterojunction NPs via a nanoprecipitation approach. (b) Energy diagram of utilized materials with highlighted possible charge and energy transfer pathways: electron transfer (1), hole transfer (2), and energy transfer (3). NHE: Normal Hydrogen Electrode. (c) Steady-state UV–Vis absorption (solid lines) and photoluminescence (dashed lines) spectra for small molecule POZ–M NPs (orange), ITIC NPs (blue), and POZ–M:ITIC NPs (green) in water.

nanoprecipitation approach,[22] where the resulting POZ-M:ITIC NPs formed a stable dispersion with a diameter of 30 nm as determined by dynamic light scattering (DLS, Fig. 2b and Fig. S4, ESI†). Powder X-Ray diffraction (PXRD) was used to study the structure morphology, specifically sample crystallinity. PXRD analysis revealed that lyophilized heterojunction NPs were crystalline, probably because ITIC tends to form crystalline layered structures (Fig. S5, ESI†). Morphology of designed NPs was further studied by cryogenic electron microscopy (Cryo-EM) that allows NPs to be envisioned in their native state. Cryo-EM micrographs showed that heterojunction NPs were spherical with well intermixed POZ-M and ITIC phases (Fig. 2a and Fig. S6a, ESI†). In contrast to pure molecular heterojunction NPs studied here, it was previously found that it is hard to achieve uniform distribution of donor and acceptor when donor polymers were mixed with molecular acceptors.[23] In order to understand the impact of the purely molecular architecture of the designed system, we have further studied photophysical properties in detail, specifically charge and energy transfer pathways of heterojunction NPs upon light illumination.
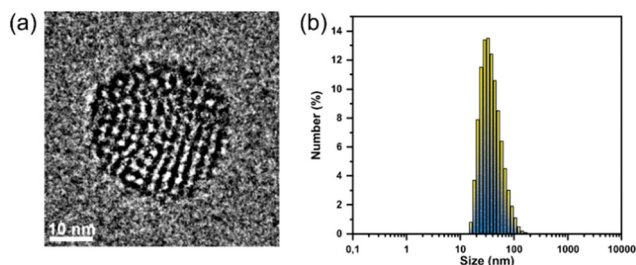
Fig. 2 (a) Cryo-EM micrograph and (b) distribution of the hydrodynamic diameter of heterojunction POZ–M:ITIC NPs.

Fig. 1b shows the energy levels of POZ-M and ITIC as determined from differential pulse voltammetry (Fig. S7 and Table S1, ESI†). The reduction potential of POZ-M ($E_{POZ-M-/POZ-M}$ = −1.47 V vs. NHE) is more negative than that of ITIC ($E_{ITIC-/ITIC}$ = −0.58 V vs. NHE). As seen from the energy diagram, POZ-M has sufficient thermodynamic driving force (0.89 V) to reduce ITIC. Moreover, both donor and acceptor molecules have favorable excited state potentials ($E_{POZ-M-/POZ-M*}$ = 0.95 V vs. NHE, $E_{ITIC-/ITIC*}$ = 1.12 V vs. NHE) that allows photogenerated holes to get regenerated by ascorbic acid. The heterojunction NPs have therefore a staggered (type II) energy alignment. Based on the energy level alignment, efficient charge separation can be achieved via either electron transfer (ET) from POZ-M to ITIC or hole transfer (HT) from ITIC to POZ-M, or a combination of both.

Light absorption within the entire visible range in pair with favorable energy/charge transfer capabilities are among the key preconditions of material utilization in solar fuel research. Fig. 1c depicts steady-state absorption spectra of NPs based on single molecules (POZ-M or ITIC), and heterojunction POZ-M:ITIC NPs. POZ-M NPs has red-shifted absorption spectrum relative to the POZ-M solution in THF (Fig. S8, ESI†). This is caused due to strong J-aggregation of POZ-M of its singular particle form.[24] The blue shifted absorption in heterojunction POZ-M:ITIC NPs as compared to POZ-M NPs alone should indicate that the POZ-M in singular nanoparticle aggregates more than it does in its heterojunction with ITIC.[25] The emission of single molecule POZ-M NPs (λ_{exc} = 495 nm) and ITIC NPs (λ_{exc} = 640 nm) is centered at 615 and 770 nm respectively (Fig. 1c). As there is a large overlap between the emission of the donor and absorption of the acceptor, energy transfer (EnT) from POZ-M to ITIC is a plausible relaxation pathway in addition to feasible ET/HT discussed above. Hereby, EnT is seen as an additional pathway that may promote exciton diffusion within chromophores.

The emission spectrum of heterojunction NPs is presented in Fig. S9 (ESI†). Under the excitation of 495 nm POZ-M can be predominantly excited. At this excitation wavelength, 92% quenching of both donor and acceptor part was observed for POZ-M:ITIC with a donor to acceptor weight ratio of 1:1. Once the ratio of ITIC in heterojunction NPs increased to 1:2 (POZ-M:ITIC), the quenching efficiency increased to 95%. Such efficient quenching of both donor and acceptor parts can be a result of (a) ET from excited POZ-M (POZ-M*) to ITIC; (b) HT from excited (ITIC*) to POZ-M; or (c) EnT from POZ-M* to ITIC, followed by HT from ITIC* to POZ-M (Fig. 1b). HT from ITIC* to POZ-M is the only possible deactivation pathway, once the heterojunction NPs are excited at 640 nm where POZ-M does not absorb. Involvement of EnT from POZ-M* and ITIC was confirmed by excitation spectrum of heterojunction NPs under the emission wavelength of 870 nm (Fig. S10, ESI†) in which the absorption region from POZ-M was covered. It is worth mentioning that such spectral overlap and quenching of both donor and acceptor parts was only observed, when both donor and acceptor were blended inside NP. Simple mixing of POZ-M NPs and ITIC NPs did not result in quenching of either donor or acceptor parts, excluding charge and energy transfer
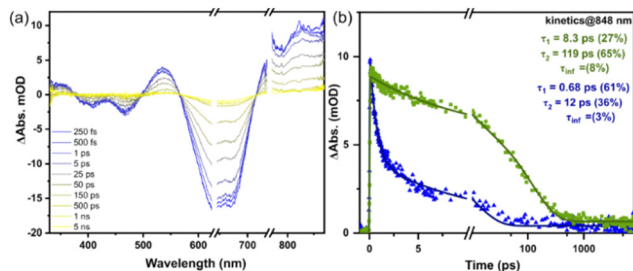
Fig. 3 (a) TA spectrum of POZ-M:ITIC heterojunction NPs excited at 640 nm. (b) Kinetic traces extracted at 848 nm for single molecule ITIC NPs (blue trace) and heterojunction NPs (green trace) excited at 640 nm.

Fig. 4 Photocatalytic production activity for single molecule POZ-M NPs (orange line), ITIC NPs (blue line) and POZ-M:ITIC NPs (95 μg, green line) initiated by LED irradiation (50 mW cm^{-2}, 420–750 nm) in the presence of 6 wt% Pt, 0.2 M ascorbic acid at pH 4 (total reaction volume 2 mL).

involvement (Fig. S10a and S10b, ESI†). This highlights that both donor and acceptor molecules need to be blended together in NP in order for both charge and energy transfer to occur.

Furthermore, we investigated energy and charge transfer processes in molecular heterojunction NPs using femtosecond transient absorption spectroscopy studies (TAS, Fig. S12 and S13, ESI†). Spectroelectrochemistry measurements were first carried out to obtain absorption features of oxidized and reduced species of POZ-M (Fig. S15, ESI†). To evidence and investigate the HT dynamics within heterojunction NPs, TAS measurements were first performed by selective excitation of the acceptor at 640 nm (Fig. 3).

The TA spectrum of POZ-M NPs under excitation of 640 nm (Fig. S14, ESI†) revealed that POZ-M molecules could not be excited under these conditions. Immediately after excitation we observed spectral signatures of charge transfer species, oxidized POZ-M (POZ-M^{+}) and reduced ITIC (ITIC$^{•-}$) in the TA spectrum of heterojunction NPs (Fig. 3). According to spectroelectrochemistry data (Fig. S15, ESI†), POZ-M^{+} has positive absorption signals centered at 330, 545, and 840 nm, and negative absorption signals centered at 405 and 465 nm respectively. At the same time, reduced acceptor molecule species ITIC$^{•-}$ appeared from 500 to 530 nm, slightly overlapping with a 545 nm shoulder from POZ-M^{+}. Observation of clear oxidized donor molecule species immediately after excitation of ITIC with a rise time below our instrument response function (IRF $\sim$200 fs) can only be a result of efficient HT from ITIC* to POZ-M. The signal at 850 nm decayed much more slowly in heterojunction POZ-M:ITIC NPs than in the neat single molecule ITIC NPs, suggesting a long-lived charge-separated state formed via HT (Fig. S16, ESI†) prior to charge recombination. TAS experiments performed under 495 nm (ESI,† Fig. S17) excitation in pair with steady-state data discussed earlier suggests the contribution of the following photophysical processes to charge separation in heterojunction NPs: (1) ultrafast EnT from POZ-M* to ITIC within IRF, followed by fast HT from ITIC* to POZ-M and (2) direct ET from POZ-M* to ITIC due to sufficient thermodynamic driving force (0.89 V). The process (1) probably dominates the charge separation once the system is excited at 495 nm since the EnT from POZ-M* to ITIC seems to be very efficient from the steady state excitation spectrum of blended NPs (Fig. S10, ESI†).
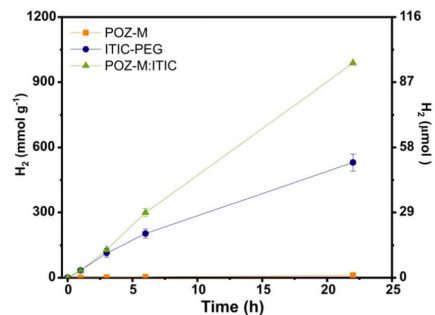
The activity of heterojunction NPs loaded with 6 wt% platinum as the H$_2$ evolution catalyst was then compared to the activity of single molecule POZ-M NPs or ITIC NPs under solar light simulating conditions (LED, 50 mW cm^{-2}, 420–750 nm) in the presence of ascorbic acid as electron donor (pH = 4). As seen from Fig. 4, heterojunction NPs had a H$_2$ production rate (63 mmol g^{-1} h^{-1}) that is 2 and 100 times higher than that for a single molecule ITIC NPs (29.5 mmol g^{-1} h^{-1}) and POZ-M NPs (0.6 mmol g^{-1} h^{-1}) respectively. Blank experiments excluding either a light harvester or a electron donor resulted in negligible H$_2$ production. The external quantum yield for POZ-M:ITIC was determined to be 0.8% at 450 nm (Fig. S18, ESI†).

The amount of produced H$_2$ by POZ-M:ITIC NPs after 22 h of illumination was 104 μmol, corresponding to hydrogen production capacity of the system, 2.4 μmol mL^{-1} h^{-1}. After 22 h of continuous H$_2$ production, no pronounced morphology change was observed for POZ-M:ITIC NPs as evidenced from Cryo-EM image recorded after photocatalysis (Fig. S6b, ESI†). The overall rates of H$_2$ production for designed molecular heterojunction NPs were among the most efficient small organic molecule based photocatalysts,[5,6,18,19] and even higher than those observed for many of the polymer-based heterojunction NPs,[16,17,26,27] and inorganic photocatalysts.[28] Having molecular donor and molecular acceptor that both can form crystalline structures, results in enhanced mixing, structure ordering and thus charge delocalization. This suggests that heterojunction structures where both donor and acceptor part are molecules have potential to achieve high charge transfer efficiencies and thus enhanced photocatalytic performance. These design principles can be further implemented not only for systems used in hydrogen evolution, but also for formation of light harvesting materials that can form various types of fuels.

A small molecular photosensitizer based on phenoxazine (POZ-M) has been synthesized and used to prepare small organic molecule heterojunction NPs with a non-fullerene molecular acceptor ITIC, rendering a hydrogen production rate of 63 mmol g^{-1} h^{-1}. Cryo-EM measurements revealed that heterojunction NPs are well blended spherical NPs. PXRD showed that the NPs have crystalline structure. Such morphology of POZ-M:ITIC NPs promoted charge separation at the interface of donor and acceptor, resulting in efficient charge separation

and energy transfer as evidenced by steady-state and transient absorption spectroscopy studies. This work provides a new strategy from molecular design approach to develop organic small molecule heterojunction photocatalytic NPs, which could be further developed and applied in water oxidation, carbon dioxide reduction, and photoredoxcatalysis for organic transformation.

Conflicts of interest

There are no conflicts to declare.

Notes and references

1 C. Dai, S. Xu, W. Liu, X. Gong, M. Panahandeh-Fard, Z. Liu, D. Zhang, C. Xue, K. P. Loh and B. Liu, *Small*, 2018, **14**, 1801839.
2 Y. Wu, X. Zhang, Y. Xing, Z. Hu, H. Tang, W. Luo, F. Huang and Y. Cao, *ACS Mater. Lett.*, 2019, **1**, 620–627.
3 A. M. Elewa, C.-Y. Liao, W.-L. Li, I. M. A. Mekhemer and H.-H. Chou, *Macromolecules*, 2023, **56**, 1352–1361.
4 J. Kosco, S. Gonzalez-Carrero, C. T. Howells, T. Fei, Y. Dong, R. Sougrat, G. T. Harrison, Y. Firdaus, R. Sheelamanthula, B. Purushothaman, F. Moruzzi, W. Xu, L. Zhao, A. Basu, S. De Wolf, T. D. Anthopoulos, J. R. Durrant and I. McCulloch, *Nat. Energy*, 2022, **7**, 340–351.
5 Y. Liang, T. Li, Y. Lee, Z. Zhang, Y. Li, W. Si, Z. Liu, C. Zhang, Y. Qiao, S. Bai and Y. Lin, *Angew. Chem., Int. Ed.*, 2023, e202217989.
6 H. Yang, C. Li, T. Liu, T. Fellowes, S. Y. Chong, L. Catalano, M. Bahri, W. Zhang, Y. Xu, L. Liu, W. Zhao, A. M. Gardner, R. Clowes, N. D. Browning, X. Li, A. J. Cowan and A. I. Cooper, *Nat. Nanotechnol.*, 2023, **18**, 307–315.
7 M. V. Pavliuk, M. Lorenzi, D. R. Morado, L. Gedda, S. Wrede, S. H. Mejias, A. Liu, M. Senger, S. Glover, K. Edwards, G. Berggren and H. Tian, *J. Am. Chem. Soc.*, 2022, **144**, 13600–13611.
8 Y. Bai, C. Li, L. Liu, Y. Yamaguchi, B. Mounib, H. Yang, A. Gardner, M. A. Zwijnenburg, N. D. Browning, A. J. Cowan, A. Kudo, A. I. Cooper and R. S. Sprick, *Angew. Chem., Int. Ed.*, 2022, **61**, e202201299.
9 S. Wang, B. Cai and H. Tian, *Angew. Chem., Int. Ed.*, 2022, **61**, e202202733.
10 W. Zhao, P. Yan, B. Li, M. Bahri, L. Liu, X. Zhou, R. Clowes, N. D. Browning, Y. Wu, J. W. Ward and A. I. Cooper, *J. Am. Chem. Soc.*, 2022, **144**, 9902–9909.
11 H. Wang, C. Yang, F. Chen, G. Zheng and Q. Han, *Angew. Chem., Int. Ed.*, 2022, **61**, e202202328.
12 W. Yu, M. V. Pavliuk, A. Liu, Y. Zeng, S. Xia, Y. Huang, H. Bai, F. Lv, H. Tian and S. Wang, *ACS Appl. Mater. Interfaces*, 2022, **15**, 2183–2191.
13 P. Gai, W. Yu, H. Zhao, R. Qi, F. Li, L. Liu, F. Lv and S. Wang, *Angew. Chem., Int. Ed.*, 2020, **59**, 7224–7229.
14 W. Yu, H. Bai, Y. Zeng, H. Zhao, S. Xia, Y. Huang, F. Lv and S. Wang, *Research*, 2022, **2022**, 9834093.
15 M. Sachs, H. Cha, J. Kosco, C. M. Aitchison, L. Francàs, S. Corby, C.-L. Chiang, A. A. Wilson, R. Godin, A. Fahey-Williams, A. I. Cooper, R. Sebastian Sprick, I. McCulloch and J. R. Durrant, *J. Am. Chem. Soc.*, 2020, **142**, 14574–14587.
16 J. Kosco, M. Bidwell, H. Cha, T. Martin, C. T. Howells, M. Sachs, D. H. Anjum, S. Gonzalez Lopez, L. Zou, A. Wadsworth, W. Zhang, L. Zhang, J. Tellam, R. Sougrat, F. Laquai, D. M. DeLongchamp, J. R. Durrant and I. McCulloch, *Nat. Mater.*, 2020, **19**, 559–565.
17 A. Liu, L. Gedda, M. Axelsson, M. Pavliuk, K. Edwards, L. Hammarström and H. Tian, *J. Am. Chem. Soc.*, 2021, **143**, 2875–2885.
18 A. Dolan, J. M. de la Perrelle, T. D. Small, E. R. Milsom, G. F. Metha, X. Pan, M. R. Andersson, D. M. Huang and T. W. Kee, *ACS Appl. Nano Mater.*, 2022, **5**, 12154–12164.
19 Y. Zhu, Z. Zhang, W. Si, Q. Sun, G. Cai, Y. Li, Y. Jia, X. Lu, W. Xu, S. Zhang and Y. Lin, *J. Am. Chem. Soc.*, 2022, **144**, 12747–12755.
20 Y. Guo, Q. Zhou, J. Nan, W. Shi, F. Cui and Y. Zhu, *Nat. Commun.*, 2022, **13**, 2067.
21 Y. Firdaus, V. M. Le Corre, S. Karuthedath, W. Liu, A. Markina, W. Huang, S. Chattopadhyay, M. M. Nahid, M. I. Nugraha, Y. Lin, A. Seitkhan, A. Basu, W. Zhang, I. McCulloch, H. Ade, J. Labram, F. Laquai, D. Andrienko, L. J. A. Koster and T. D. Anthopoulos, *Nat. Commun.*, 2020, **11**, 5220.
22 M. V. Pavliuk, S. Wrede, A. Liu, A. Brnovic, S. Wang, M. Axelsson and H. Tian, *Chem. Soc. Rev.*, 2022, **51**, 6909–6935.
23 S. Liang, S. Li, Y. Zhang, T. Li, H. Zhou, F. Jin, C. Sheng, G. Ni, J. Yuan, W. Ma and H. Zhao, *Adv. Funct. Mater.*, 2021, **31**, 2102764.
24 Y. Deng, W. Yuan, Z. Jia and G. Liu, *J. Phys. Chem. B*, 2014, **118**, 14536–14545.
25 K. Kong, S. Zhang, Y. Chu, Y. Hu, F. Yu, H. Ye, H. Ding and J. Hua, *Chem. Commun.*, 2019, **55**, 8090–8093.
26 Z. Zhang, W. Si, B. Wu, W. Wang, Y. Li, W. Ma and Y. Lin, *Angew. Chem., Int. Ed.*, 2022, **61**, e202114234.
27 J. Kosco, S. Gonzalez-Carrero, C. T. Howells, W. Zhang, M. Moser, R. Sheelamanthula, L. Zhao, B. Willner, T. C. Hidalgo, H. Faber, B. Purushothaman, M. Sachs, H. Cha, R. Sougrat, T. D. Anthopoulos, S. Inal, J. R. Durrant and I. McCulloch, *Adv. Mater.*, 2021, 2105007.
28 B. H. Lee, S. Park, M. Kim, A. K. Sinha, S. C. Lee, E. Jung, W. J. Chang, K. S. Lee, J. H. Kim, S. P. Cho, H. Kim, K. T. Nam and T. Hyeon, *Nat. Mater.*, 2019, **18**, 620–626.